SUPPLEMENTAL INFORMATION

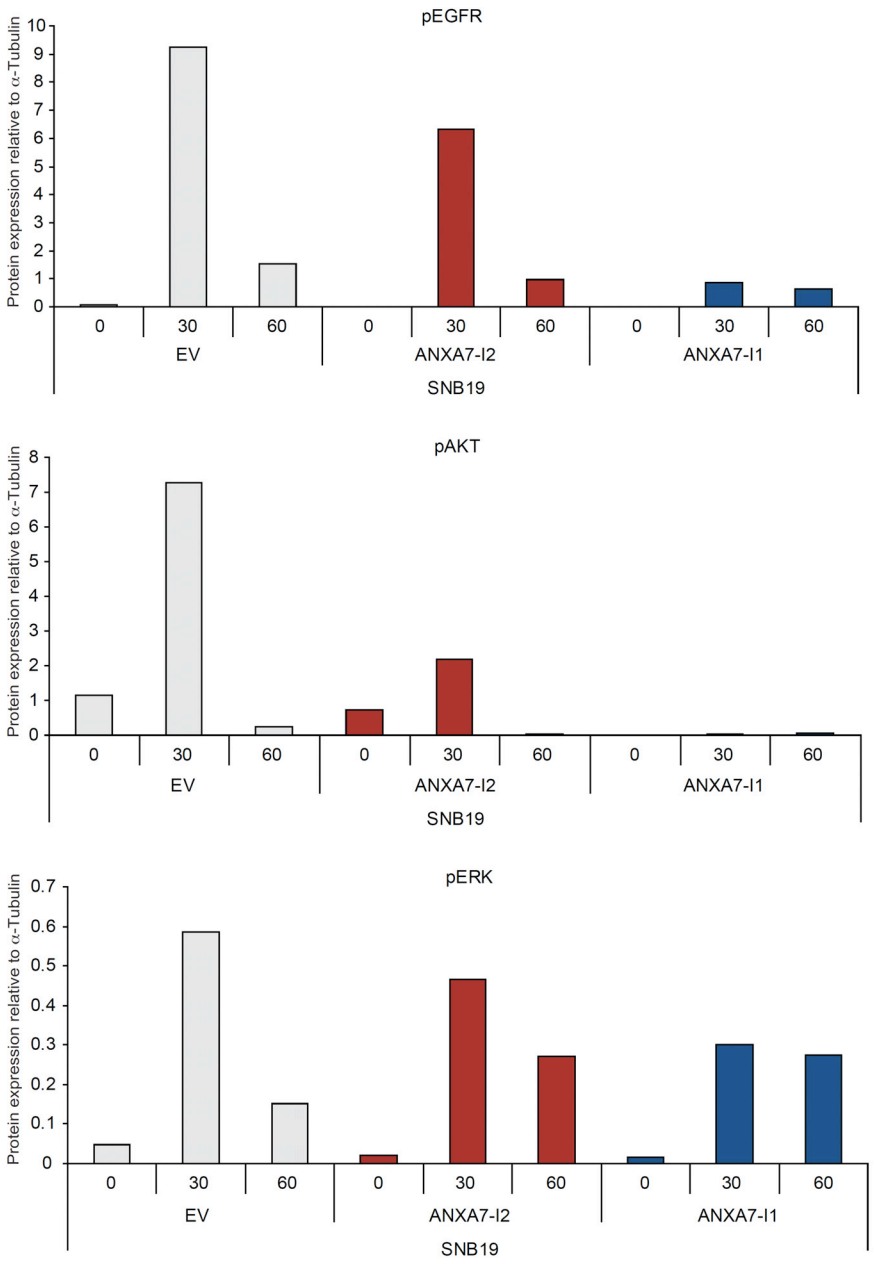

Figure S1. pEGFR, pAKT and pERK1/2 Protein Quantification
Quantification of the phosphoprotein bands from the immunoblotting analysis shown in **Fig. 1E**. Protein quantities are expressed relative to α-Tubulin expression.

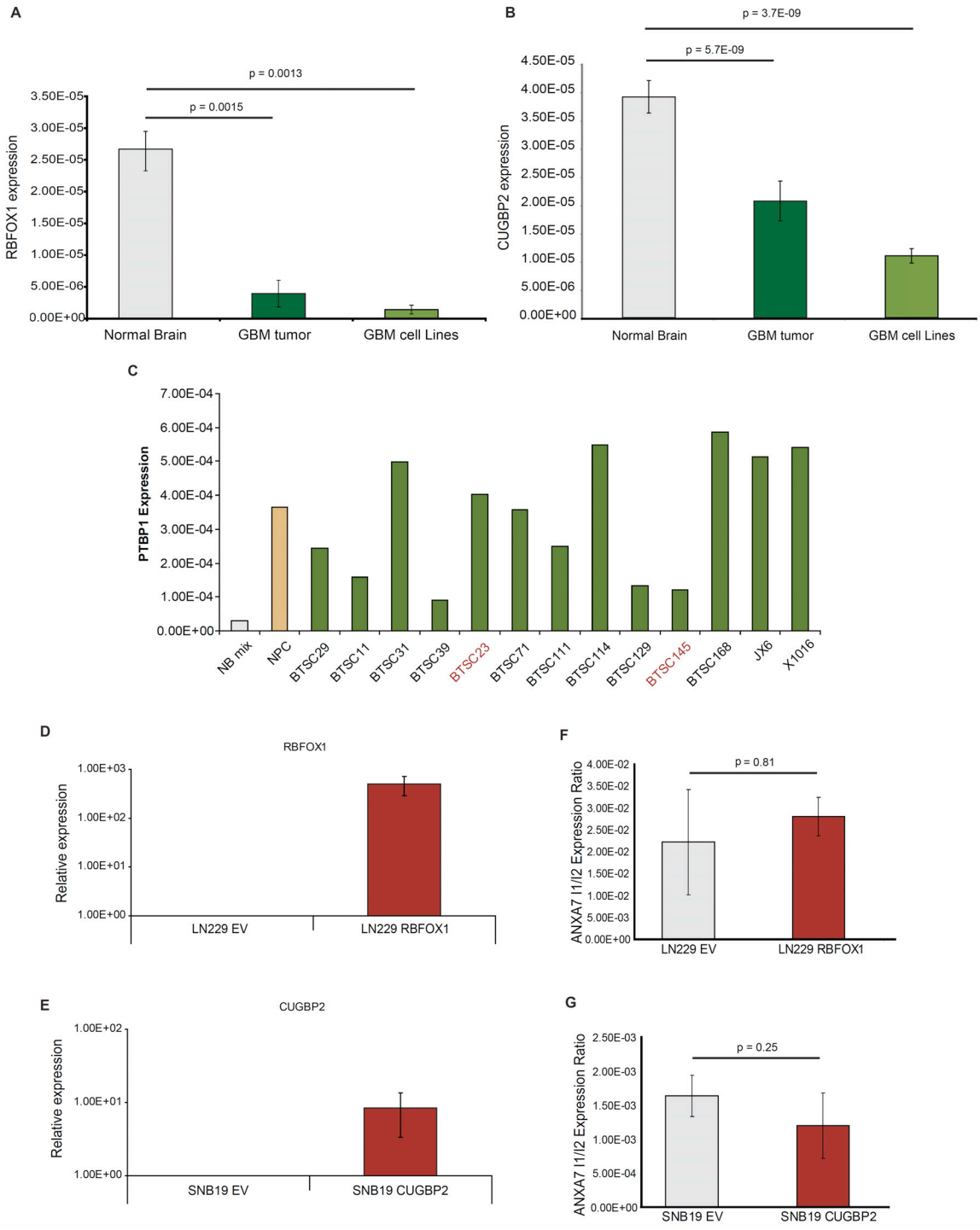

Figure S2. RBFOX1 and CUGBP2 Do Not Regulate ANXA7 Splicing

A-**B**, average expression of RBFOX1 (**A**) and CUGBP2 (**B**) mRNA in normal brain cortex, glioblastoma (GBM) tumors, and GBM-derived cell cultures measured by qRT-PCR; n = 8 (normal brain cortex), *n* = 7 (GBM tumors), and *n* = 13 (GBM-derived cell cultures); error bars represent mean ± s.d. **C**, qRT-PCR analysis of PTBP1 mRNA expression in pooled normal brain (NB mix), neural precursor cells (NPC), patient-derived brain tumor stem cells (BTSC), and patient-derived GBM cells (JX6 and X1016).**D**-**E**, qRT-PCR analysis of RBFOX1 (**D**) or CUGBP2 (**E**) after their overexpression in LN229 and SNB19 cell lines, respectively;. *n* = 3 independent clones for each overexpression experiment; error bars represent mean ± s.d. **F**-**G**, qRT-PCR analysis of changes in ANXA7I1/I2 mRNA ratio upon RBFOX1 overexpression in LN229 cells (**F**) and CUGBP2 overexpression in SNB19 cells (**G**). *n* = 7 independent experiments for LN229 RBFOX1; *n* = 4 independent experiments for all other samples; error bars represent mean ± s.d.

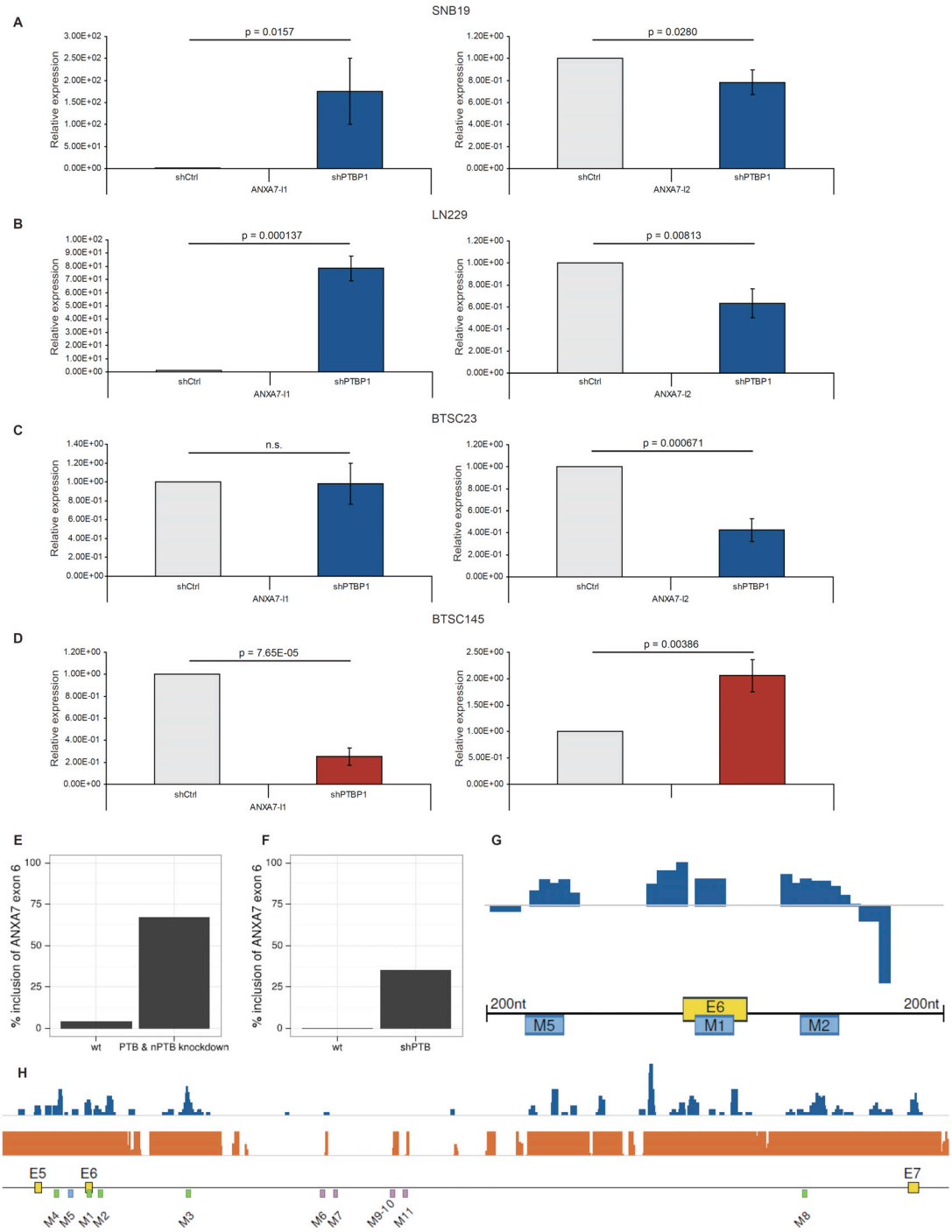

Figure S3. PTBP1 mediates ANXA7 Exon 6 Splicing

A-D, qRT-PCR analysis showing changes in ANXA7-I1 and ANXA7-I2 mRNA upon lentiviral PTBP1 silencing (or shCtrl) in SNB19 (**A**), LN229 (**B**), BTSC23 (**C**) cells, characterized by high PTBP1 expression levels, and upon lentiviral overexpression of PTBP1 in BTSC145 cells with low endogenous PTBP1 expression (**D**). (**E**) Re-analysis of data from Llorian et al. (55) showing increase of ANXA7 exon 6 inclusion from 3.9% to 67% upon PTB and nPTB knockdown. (**F**) Re-analysis of data from Xue et al. (58) showing increase of ANXA7 exon 6 inclusion from 0% to 35.3% upon PTB knockdown. (**G**) Re-analysis of PTB next-generation SELEX data from Reid et al. (57) revealing correspondence with three of our predicted PTBP1 binding-sites (M1, M2, and M5). (**H**) Re-analysis of PTB CLIPseq data by Xue et al. (58) revealing overlap with five of our predicted binding sites. The blue lane shows PTB CLIP peaks from Xue et al. (56) for ANXA7 exons 5 to 7. The brown lane shows the Encode Mapability track (50 nt). PTBP1 binding sites predicted in our analysis are shown in the bottom panel, the five overlapping predicted sites (M1, M2, M3, M4 and M8) are indicated in green. Five of the sites selected for mutational analysis also show peaks in the CLIP analysis (shown in green). Four of the sites selected for mutation are in regions of low mapability (shown in purple).

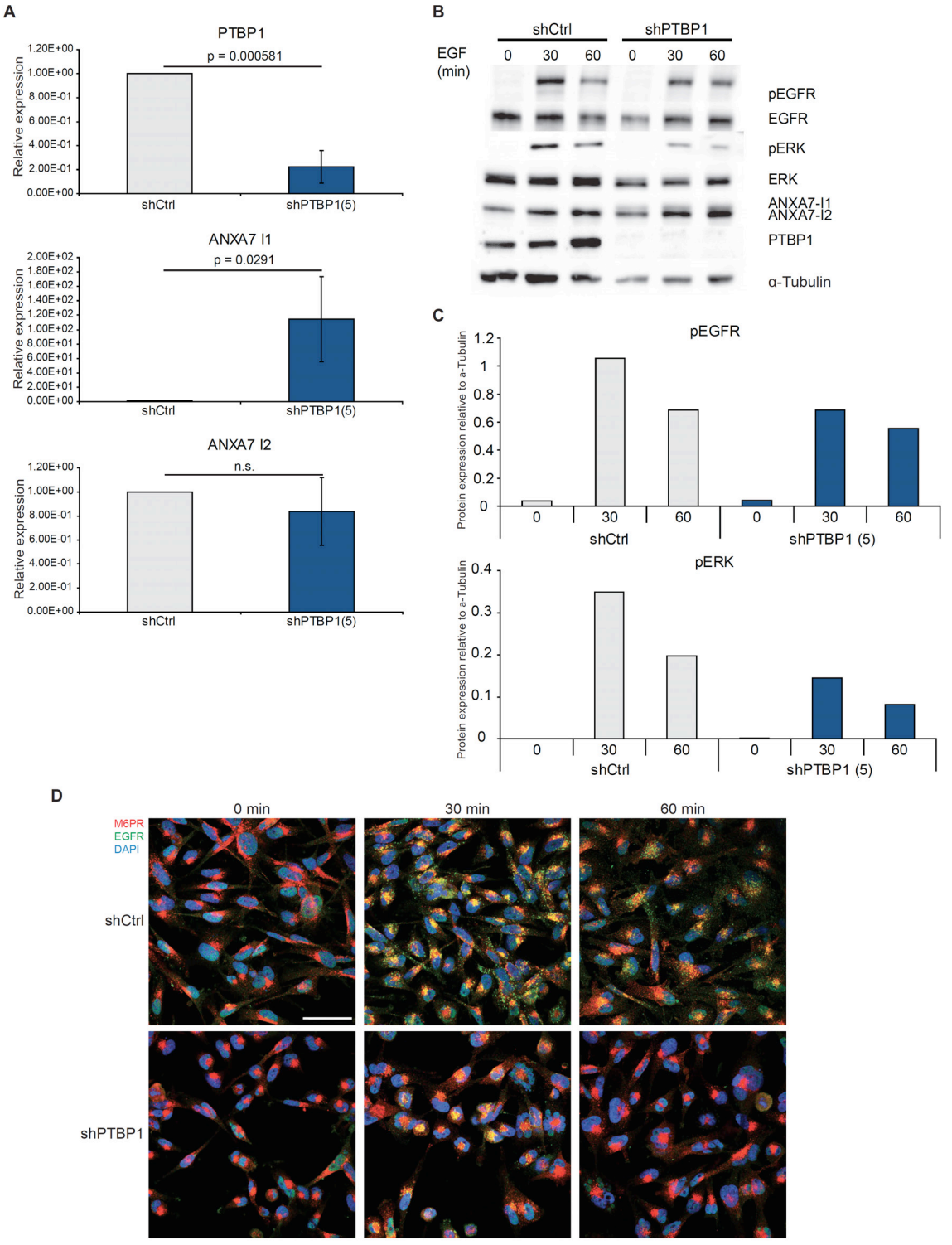

Figure S4. PTBP1 Effect on EGFR Signaling Through ANXA7 Confirmed By a Second shRNA Sequence Targeting PTBP1. **A,** qRT-PCR analysis showing changes in PTBP1, ANXA7-I1 and ANXA7-I2 mRNA upon lentiviral PTBP1 silencing (or shCtrl) in SNB19. **B-C**, time-course of EGFR pathway activation upon EGF stimulation in SNB19-shCtrl and SNB19-shPTBP1 cells in immunoblotting analysis (**B**) and relative (to α-Tubulin) phosphoprotein quantification (**C**). **D**, Early (EEA1) and late (M6PR) endosomal marker co-immunostaining with EGFR in EGF-stimulated SNB19-shCtrl and SNB19-shPTBP1; nuclei counterstained with DAPI. Scale bar is 50 μm.

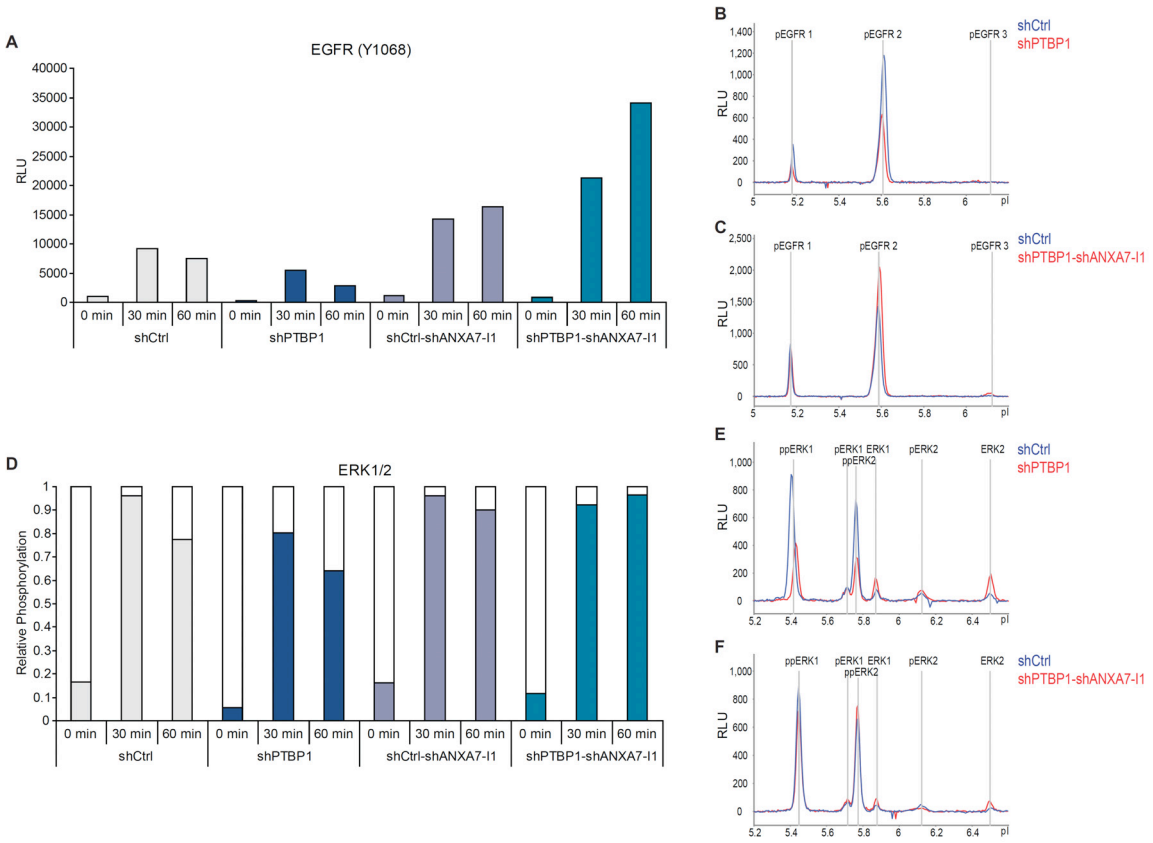

Figure S5. Probed Isoelectric Focusing (PIF) Confirms the Effect of PTBP1 on EGFR Signaling
A-C, PIF analysis showing differential EGFR phosphorylation in SNB19-shCtrl, SNB19-shPTBP1, SNB19 shANXA7-I1 and SNB19 shPTBP1 shANXA7-I1, shown as quantification in a time-course of the phosphorylated protein (**A**) and as a comparison of the single phosphorylation peaks of SNB19 shPTBP1 (**B**) and SNB19 shPTBP1 shANXA7-I1 (**C**), both relative to SNB19 shCtrl, after a 30-minute EGF stimulation. **D-F**, PIF analysis showing differential ERK1/2 phosphorylation in SNB19-shCtrl, SNB19-shPTBP1, SNB19 shANXA7-I1 and SNB19 shPTBP1 shANXA7-I1, shown as relative quantification in a time-course of the phosphorylated protein (**D**) and as a comparison of the single phosphorylation peaks of SNB19 shPTBP1 (**E**) and SNB19 shPTBP1 shANXA7-I1 (**F**), both relative to SNB19 shCtrl, after a 30-minute EGF stimulation.

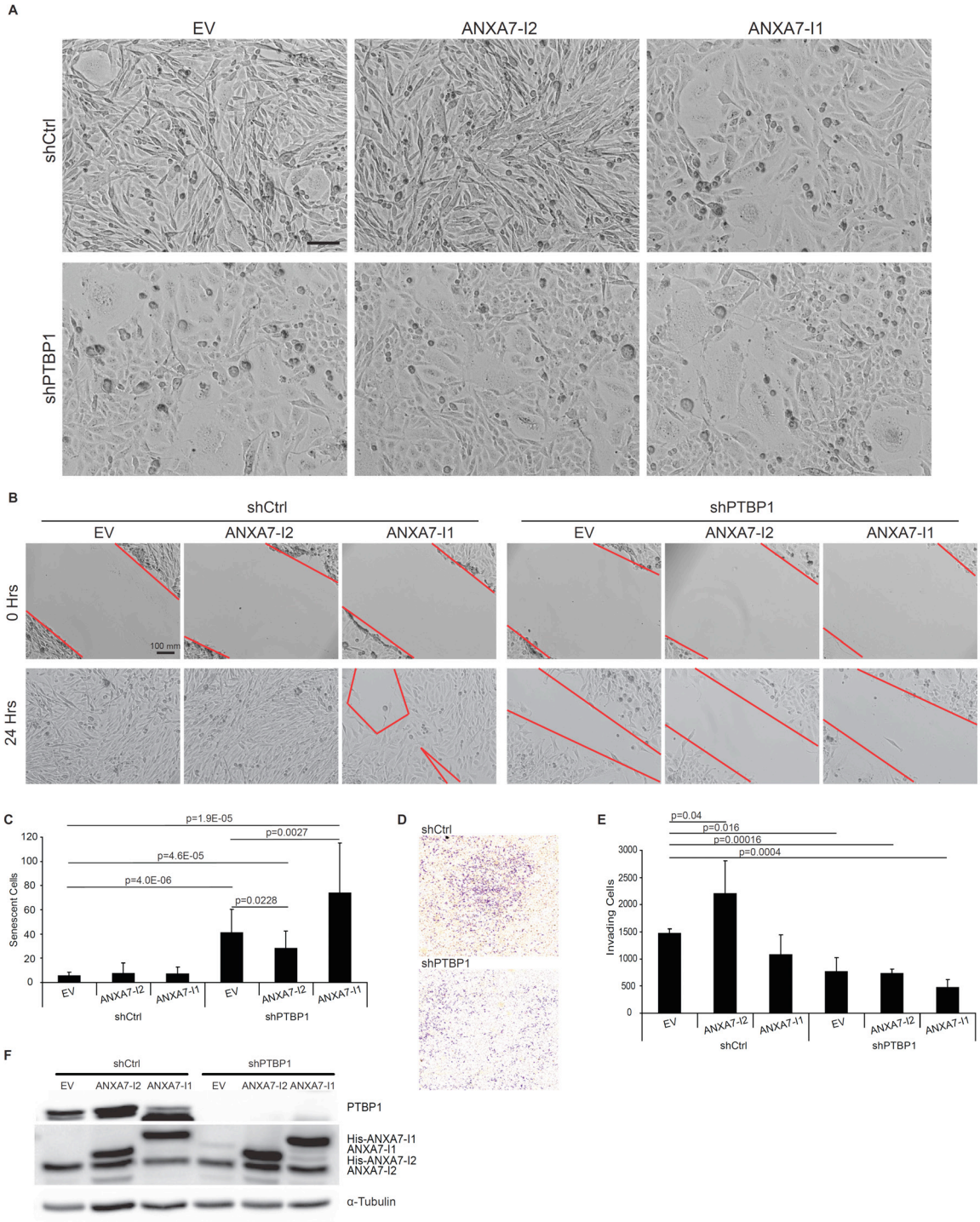

Figure S6. PTBP1 Knockdown Enhances Cell Senescence and Inhibits Cell Migration and Invasion *In Vitro*
A, microphotographs of SNB19-shCtrl and SNB19-shPTBP1 cells transduced with lentivirus to express EV, ANXA7-I2 or ANXA7-I1. Scale bar is 100 μm. **B**, wound healing assay of SNB19 cells infected as in (**A**) showing a reduced ability of SNB19-shPTBP1 cells and SNB19-shCtrl-ANXA7-I2 to cover the scratch. Scale bar is 100 μm. **C**, measurement of (senescence-associated) β-gal positive cells in cells infected as in (**A**); *p* values according to unpaired *t*-test; $n = 10$ for SNB19-shC-EV; $n = 20$ for SNB19-shPTBP1-EV; $n = 19$ for all other samples; error bars represent mean ± s.d. **D**-**E**, representative microphotographs (**D**) of invading SNB19-shCtrl and SNB19-shPTBP1 cells in a Matrigel assay and corresponding quantification (**E**) of invading cells infected as in (**A**); *p* values according to unpaired *t*-test; $n = 4$; error bars represent mean ± s.d. **F**, western blot analysis showing the expression of PTBP1, ANXA7-I1 and ANXA7-I2 in the SNB19 cells infected as in (**A**).

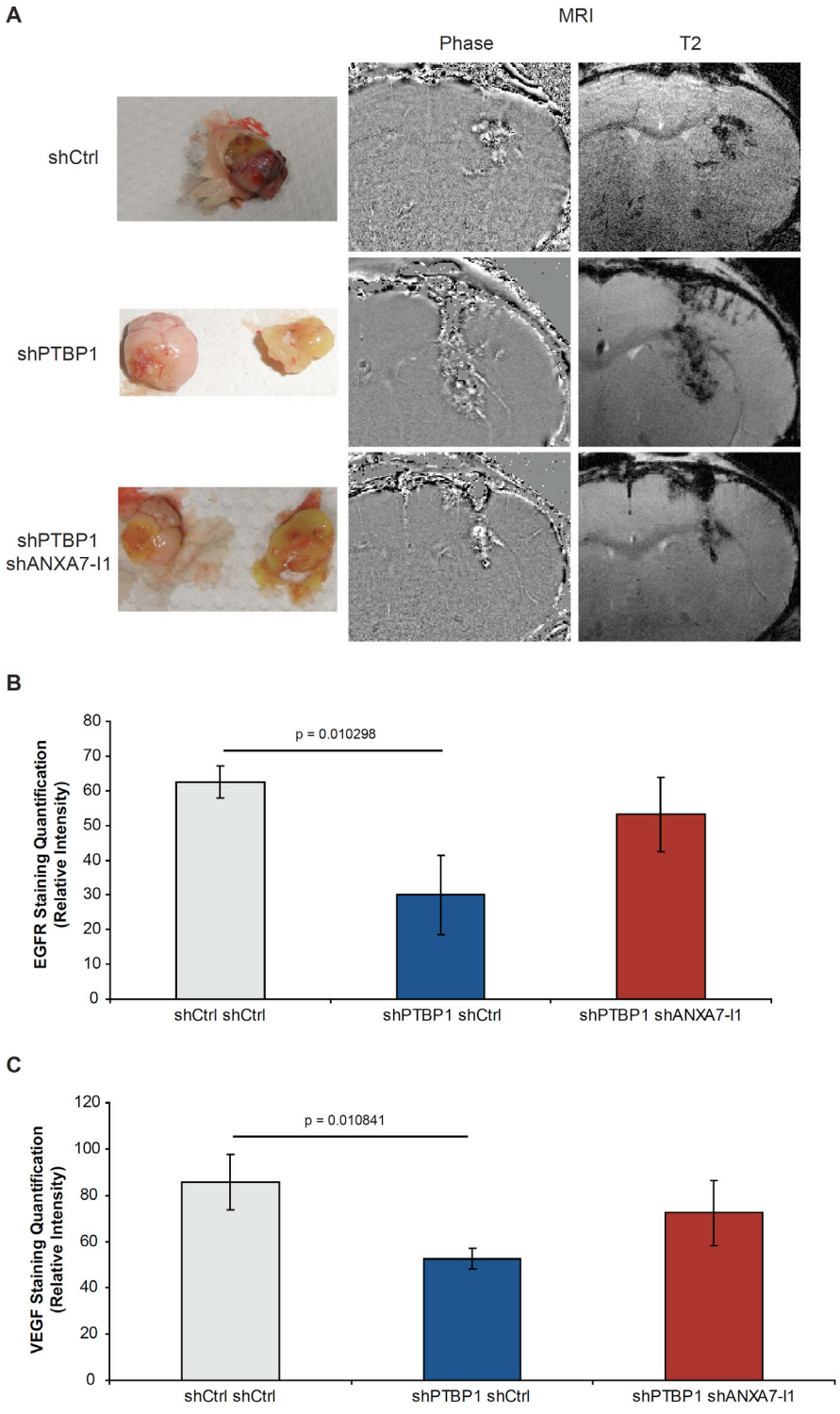

Figure S7. Gross Tumor Morphology and MRI-based confirmation of striatal injection
A, Representative gross tumor images of orthotopic intracranial tumors derived from SNB19 cells with PTBP1 knockdown, PTBP1/ANXA7-I1 double-knockdown, and control cells, where the tumor portion growing in the subarachnoid space is detached from the brain (first column) and Magnetic Resonance Imaging (MRI) (Phase imaging, second column; T2-weighted imaging, third column) showing the injection site localized in the striatum of NOD/SCID mice of SNB19 shCtrl, shPTBP1 or shPTBP1 shANXA7-I1. **B-C,** Quantification of EGFR (**B**) and VEGF (**C**) signal intensity from immunostainings shown in **Fig. 4B**; *n* = 3 for each group; error bars represent mean ± s.d.

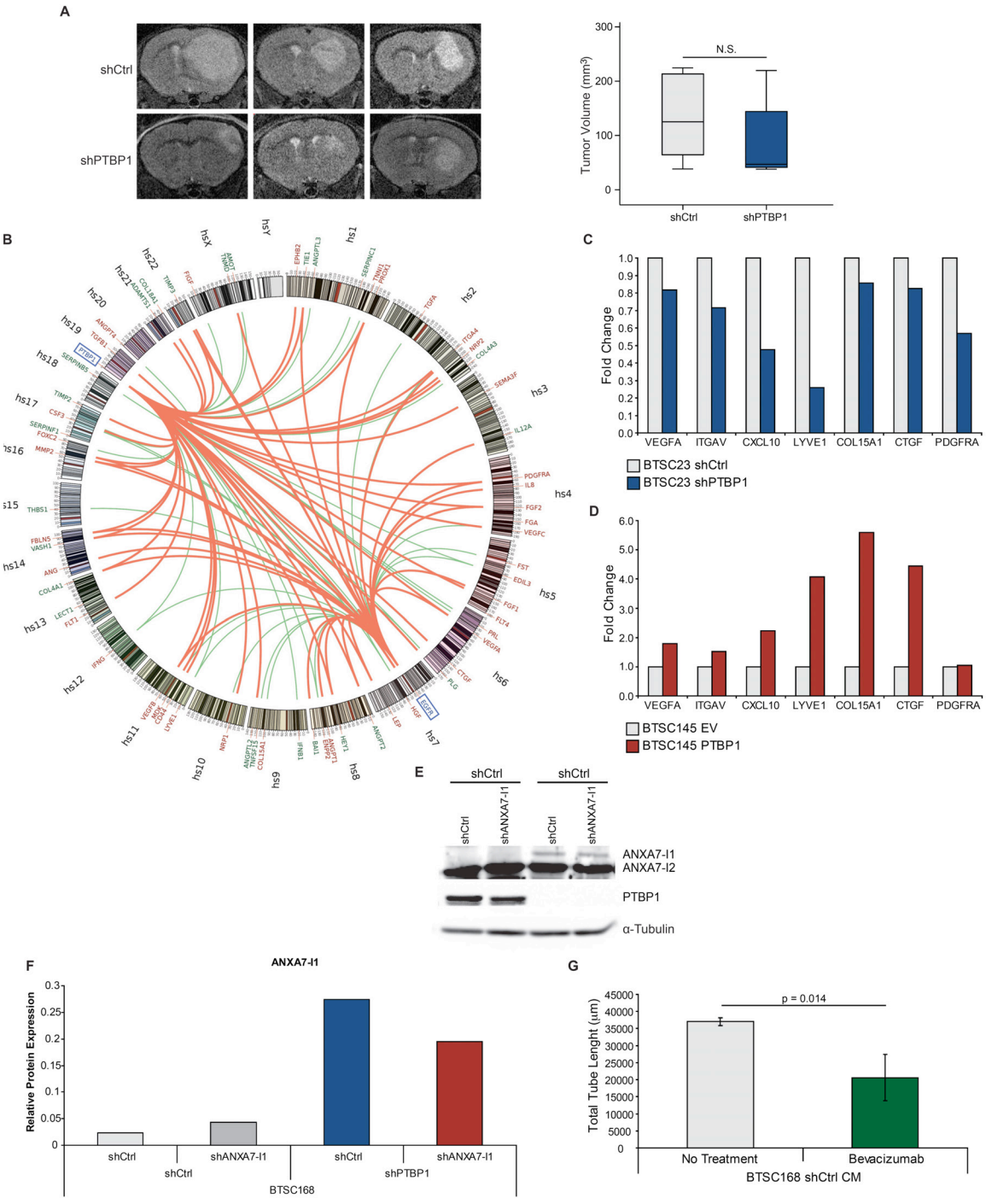

Figure S8. Role of PTBP1 in Regulating Tumor Angiogenesis

A, T2-weighted MR images of representative tumors resulting from BTSC23 cells after lentiviral knockdown of PTPB1 (shPTBP1) or control knockdown with scrambled, non-targeting shRNA (shCtrl) and intracranial injection into the brain of NOD/SCID mice. The graph shows the measurement of tumor volumes in tumors originating from BTSC23-shPTBP1, $n = 5$ and BTSC23-shC cells, $n = 7$; box plots show the smallest and largest observations (upper and lower whiskers, respectively), the interquartile range (box), and the median (black line). Data points more than 1.5 times the interquartile range lower than the first quartile or 1.5 times the interquartile range higher than the third quartile were considered to be outliers. **B**, circos circular genome structure mapping of co-regulated expression of PTBP1 with multiple angiogenesis genes (false-discovery rate adjusted $q < 0.001$), most of which also show co-regulation with EGFR; result based on analysis in 550 glioblastomas; red and green labels denote pro-angiogenic and anti-angiogenic genes, respectively; red and green edges denote positive and negative correlations, respectively. **C-D**, qRT-PCR validation analysis of change in expression of seven EGFR-regulated angiogenesis genes in BTSC23 cells (with high endogenous PTBP1 expression) after

lentiviral PTBP1 knockdown and corresponding control cells infected with non-targeting shRNA (**C**), and in BTSC145 cells (with low endogenous PTBP1 expression) after lentiviral re-expression of PTBP1 and corresponding control cells infected with empty control vector (EV) (**D**). **E**, immunoblotting analysis showing the expression of PTBP1, ANXA7-I1 and ANXA7-I2 in BTSC168 cells used in an endothelial cell (EC) tube formation assay in **Fig. 5C** and **Panel G** and lentivirally infected with shPTBP1 and shANXA7-I1, as single or double infection, and respective controls. **F**, quantification of the ANXA7-I1 bands from the immunoblotting analysis shown in (**E**). Protein quantities are expressed relative to α-Tubulin expression. **G**, EC tube formation assay; quantification of the total length of the tubes observed in each well after a 24-hour incubation with medium conditioned (CM) by BTSC168 control cells upon Bevacizumab treatment; $n = 9$ independent samples; error bars represent mean ± s.d.

Table S1. Role of PTBP1 in Tumor Angiogenesis and Relationship to EGFR

A: Results of Co-Regulation Analysis (Figure S3)

Positive Correlation		Negative Correlation	
PTBP1	**EGFR**	**PTBP1**	**EGFR**
Activators		**Activators**	
PROX1		FIGF	
ITGA4		TNNI1	
PDGFRA		FGA	
FGF2		EDIL3	
FGF1		PRL	
VEGFA		HGF	
CTGF		ENPP2	
LEP		LYVE1	
CD44		IFNG	
MDK		FOXC2	
VEGFB		ANGPT4	EPHB2
FBLN5			TGFA
MMP2			NRP2
FOXC2			VEGFC
TGFB1	ANGPT1		FST
EPHB2	ANG		NRP1
NRP2			CSF3
SEMA3F		**Inhibitors**	
VEGFC		IFNB1	
COL15A1		TNFSF15	
NRP1		SERPINF1	
FLT1		SERPINB5	
CSF3		TNMD	COL18A1
Inhibitors		AMOT	THBS1
TIMP3		ANGPTL3	
TIE1		SERPINC1	
ANGPT2		COL4A3	
HEY1			
COL4A1			
VASH1			
ADAMTS1	TNMD		
COL18A1	IL12A		
COL4A3	IL8		
PLG	BAI1		
ANGPTL2	LECT1		
THBS1			
TIMP2			

B: Results of Angiogenesis Taqman Array

Upregulated genes	
Activators	**Fold Change**
LEP	7.746400002
PDGFB	8.306714672
VEGFC	9.102797582
S1PR1	2.021676273
Inhibitors	**Fold Change**
TNFSF15	3.898686095
SERPINB5	7.99540991

Downregulated genes	
Activators	**Fold Change**
GUSB	0.478085979
EPHB2	0.478592933
HGF	0.471358941
TGFB1	0.480850059
VEGFA	0.486668735
CTGF	0.479923712
CXCL10	0.115757374
CEACAM1	0.495462578
ITGAV	0.47437997
LYVE1	0.053352586
COL15A1	0.488254078
HSPG2	0.479357862
F2	0.11832403
GRN	0.458853335
ITGB3	0.473931678
PDGFRA	0.48830383
Inhibitors	**Fold Change**
PLG	0.133947077
ANGPT2	0.482356596
PF4	0.144163715
VASH1	0.48254052
COL4A1	0.464039011
COL4A2	0.477329697
BAI1	0.486944752

C: Comparison of Results of A and B (Figure 5D-E)

Positive correlation w/ PTBP1 **AND** EGFR Downregulated in shPTBP1 Taqman Array
VEGFA CTGF PDGFRA ANGPT2 VASH1
Negative correlation w/ PTBP1 **AND** EGFR Upregulated in shPTBP1 Taqman Array
TNFSF15 SERPINB5
Positive correlation w/ PTBP1 **AND** EGFR Upregulated in shPTBP1 Taqman Array
LEP
Negative correlation w/ PTBP1 **AND** EGFR Downregulated in shPTBP1 Taqman Array
HGF LYVE1

Activators
Inhibitors

Table S2. qRT-PCR primers used for validation of angiogenesis genes

Gene:	Forward Primer:	Reverse Primer:
VEGFA	AGGGCAGAATCATCACGAAGT	GCTGCGCTGATAGACATCCA
ITGAV	ATCTGTGAGGTCGAAACAGGA	TCCAATGGTACAATGGGGCAC
CXCL10	GTGGCATTCAAGGAGTACCTC	TGATGGCCTTCGATTCTGGATT
LYVE1	AGGCTCTTTGCGTGCAGAA	CACAAGGGTGATCCCCATAATTC
COL15A1	TCATCCCATCCACCTTCTTCA	CTGGCTCCGTGTAGTAGAGGA
CTGF	GGCAAAAAGTGCATCCGTACT	CCGTCGGTACATACTCCACAG
PDGFRA	TTGAAGGCAGGCACATTTACA	GCGACAAGGTATAATGGCAGAAT
18S	CGCCGCTAGAGGTGAAATTC	CTTTCGCTCTGGTCCGTCTT

Table S3. Primers used for site-directed mutagenesis

Mutant:	Mutated sequence:	Primers:	
ANXA7 M1	tctttttcttcctatcctTttttcGctccGgtttAtttg	**Fwd**	5'-aatacagattctttttcttcctatccttttttcgctccggtttatttggattatagcagtgaagtgagtaa-3'
		Rev	5'-ttactcacttcactgctataatccaaataaaccggagcgaaaaaaggataggaagaaaaagaatctgtatt-3'
ANXA7 M2	tgtttctgattctcatgtacttgtctctcactacGtGAt	**Fwd**	5'-ctcatgtacttgtctctcactacgtgataagggctcacctgtatctattt-3'
		Rev	5'-aaatagatacaggtgagcccttatcacgtagtgagagacaagtacatgag-3'
ANXA7 M3	tctagtctatatctGctgcctActagaccagcggtctctctct	**Fwd**	5'-agaagattctagtctatatctgctgcctactagaccagcggtct-3'
		Rev	5'-agaccgctggtctagtaggcagcagatatagactagaatcttct-3'
ANXA7 M4	aaagtGtttacttctgatagactccatactttctttggt	**Fwd**	5'-ttatagtaatggaagactaaagtgtttacttctgatagactccatac-3'
		Rev	5'-gtatggagtctatcagaagtaaacactttagtcttccattactataa-3'
ANXA7 M5	acctggggtcttggttttagttAtttttcctcGtccAGg	**Fwd**	5'-ttaacctggggtcttggttttagttatttttcctcgtccaggcccttaccagca-3'
		Rev	5'-tgctggtaagggcctggacgaggaaaaatAactaaaaccaagaccccaggttaa-3'
ANXA7 M6	gatggtagtttTtttAgccgtgcagaagctAtttggttt (2 steps required)	**Fwd**	5'-cctgttcactctgatggtagttttttagccgtgcagaag-3'
		Rev	5'-cttctgcacggctaaaaaaactaccatcagagtgaacagg-3'
		Fwd'	5'-cttttgccgtgcagaagctatttggtttaattagatccca-3'
		Rev'	5'-tgggatctaattaaaccaaatagcttctgcacggcaaaag-3'
ANXA7 M7	tccttgccgatgcttatgtcctgaatggtattgcctaggttttTttA tagggtttttatggGtttagatctaacattta (2 steps required)	**Fwd**	5'-cttatgtcctgaatggtattgcctaggttttttatagggtttttatggttt-3'
		Rev	5'-aaaccataaaaaccctataaaaaaaacctaggcaataccattcaggacataag-3'
		Fwd'	5'-ctaggttttcttctagggtttttatgggtttagatctaacatttaagtctttaat-3'
		Rev'	5'-attaaagacttaaatgttagatctaaacccataaaaaccctagaagaaaacctag-3'
ANXA7 M8	cagttgtctcaatgatgCccAtttGcAggAGcaggatca	**Fwd**	5'-tcagtttcaccagttgtctcaatgatgcccatttgcaggagcaggatcaaatccagaatgcaatgttg-3'
		Rev	5'-caacattgcattctggatttgatcctgctcctgcaaatgggcatcattgagacaactggtgaaactga-3'
ANXA7 M9	ttcttcctatccatgagAatggGatgtAcAtgttAAtcc	**Fwd**	5'-attttcacgatattgattcttcctatccatgagaatgggatgtacatgttaatccatttgtttgtgtccttttttatttcgttga-3'
		Rev	5'-tcaacgaaataaaaaaggacacaaacaaatggattaacatgtacatcccattctcatggataggaagaatcaatatcgtgaaaat-3'
ANXA7 M10	ttAtGcctatccatgagcatggaatgttcttgttcttcc	**Fwd**	5'-gcagtatggccattttcacgatattgattatgcctatccatgagcat-3'
		Rev	5'-atgctcatggataggcataatcaatatcgtgaaaatggccatactgc-3'
ANXA7 M11	gcttcctatgtattttattAtAtttgaagcgattgtgag	**Fwd**	5'-ccttgtaagttggcttcctatgtattttattatatttgaagcgattgtgag-3'
		Rev	5'-ctcacaatcgcttcaaatataataaaatacataggaagccaacttacaagg-3'

EXTENDED METHODS

Clinical Samples and Genome-Wide Profiling

Clinical glioblastoma and normal brain samples from seizure surgery were collected at Stanford University, Northwestern University, and University of Freiburg under institutional review board (IRB)-approved guidelines. Written informed consent was obtained from all patients. Genomic DNA was prepared using the All Prep DNA/RNA Protein Mini Kit (Qiagen) and subjected to genomic copy number analysis using the SNP6 platform (Affimetrix) according to the manufacturer's instructions. SNP6 data analysis was performed with the Chromosome analysis Suite software (Affymetrix). 537 glioblastoma samples collected as part of The Cancer Genome Atlas (TCGA) Pilot Project (http://cancergenome.nih.gov/) were used as a discovery set. Raw Affymetrix Genome-Wide Human SNP Array 6.0 and Agilent Human Genome CGH Microarray 244A gene dosage data, Affymetrix Human Genome U133 Plus 2.0 Array and Agilent 244K Custom Gene Expression data, and Affymetrix Human Exon 1.0 ST Array exon-specific expression data, and clinical data were retrieved from the Open-Access and Controlled-Access Data Tiers Portal (https://tcga-data.nci.nih.gov/tcga/) of TCGA upon National Human Genome Research Institute (NHGRI) approval and pre-processed for downstream analyses. Gene-level copy number variation (CNV) data estimated using the Genomic Identification of Significant Targets in Cancer (GISTIC2) algorithm (1) were retrieved from the Broad Institute athttp://gdac.broadinstitute.org/ runs/analyses__ 2012_03_21/data/GBM/20120321/. Genes mapped onto the human genome coordinates using the University of Santa Cruz (UCSC) cgData HUGO probeMap were visualized using the UCSC Cancer Genomics Browser (https://genome-cancer.ucsc.edu/).

Cell Lines and Culture Conditions

SNB19, LN229, and human glioblastoma-derived cells (MB), HEK 293T cells, and Phoenix cells were grown in DMEM with 10% FBS. Primary glioblastoma-derived BTSCs were prepared from tumor specimens collected at the University of Freiburg and grown as neurospheres in Neurobasal medium (Invitrogen) containing B27 supplement (Invitrogen), FGF (20 ng/ml, R&D Systems), EGF (20 ng/ml, R&D Systems), LIF (10 ng/ml, Genaxxon biosciences), Heparin (2 μg/ml, Sigma) and glutamax (Invitrogen).

Isolation and Culture of Normal Glial Progenitor Cells.

Normal (NM), non-neoplastic cells were derived from patient tissue specimens of neurosurgical resection in accordance with a Cleveland Clinic Institutional Review Board-approved protocol. Informed consent was obtained by the tissue bank, which provided de-identified excess tissue to the laboratory immediately following surgical resection. Primary surgical tissue was collected from cortices distal to the ictal (epileptic foci) region. Tissue was dissociated for primary cell culture with a Papain dissociation kit (Worthington). Cells with the ability to proliferate were selected for in culture over 2 passages. Cells were cultured adherently in media containing 50% Neurobasal medium (Gibco) and 50% Dulbecco's modified Eagle medium (DMEM) with B27 (without vitamin A, Invitrogen, basic fibroblast growth factor (10 ng/ml), epidermal growth factor (10 ng/ml), sodium pyruvate and L-glutamine, and 5% FBS. All cultured cells were used within five passages of dissociation.

Sorting and Characterization of Glial Progenitor Cells

Single cells were sorted using anti-A2B5 MicroBeads (130-093-388, Miltenyi Biotec) according to manufacturer's protocol. In brief, live cells were incubated first with FcR Blocking Reagent (Miltenyi) for 10 mins then A2B5 antibody for 15 min at 4ºC (2.5 μg A2B5 antibody per million cells). Cells positive for A2B5 were double enriched by passing through magnetic field (MACS Separator) twice. A2B5-positive and A2B5-negative cells were characterized for nestin, GFAP, Nestin, Sox1, Sox2 and neuronal Tuj1 expression by immunofluorescence staining.

Transfection and Viral Infection

ANXA7-I1 and ANXA7-I2 were overexpressed using a retroviral vector (pBabe) or a lentiviral vector (pLV-eGFP, kindly provided by V. Baekelandt, Katholieke Universiteit Leuven) in frame with a His tag. For PTBP1 overexpression, the PTBP1 coding sequence was cloned in pLV-eGFP in frame with a FLAG tag. Knockdown of PTBP1 and ANXA7-I1 was obtained with shRNA lentiviral vectors (pGIPZ, Open Biosystems). The following clones and sequence were used: PTBP1: V3LHS_362177, ANXA7-I1: V2HS_222562. Knockdown of PTBP1 was obtained with a second shRNA lentiviral vector (pLKO, Sigma): TRCN0000231418. To infect SNB19 cells, Polybrene 8 μg/ml (Sigma) was added to the lentiviral particles. Selection of infected cells was conducted with 2 μg/ml of Puromycin (Sigma). To infect BTSCs, supernatant from transfected 293T cells was ultracentrifuged to produced high-titer, serum-free virus. A retroviral vector expressing A2BP1 (pWZL-FLAG-Fox1, kindly provided by A. Krainer, Cold Spring Harbor Laboratory) and a vector expressing FLAG-CUGBP2 (pCDNA-FLAG-CUGBP2,

kindly provided by K. Xu, University of Georgia) were used in overexpression experiments. Ectopic protein expression was determined by immunoblotting with anti-His and anti-FLAG M2 antibodies (Sigma). For miR-124 transfection in SNB19 cells, the precursor form of miR -124 (MIMAT0000422) and a scramble negative control (CN-00100001-05) were purchased from Thermo Scientific and used at a concentration of 18 nM using Lipofectamine RNAiMAX reagent (Life Technologies), as recommended by the manufacturer.

Quantitative Real-Time PCR and Angiogenesis Array

RNA was prepared using the RNeasy kit or the All Prep DNA/RNA Protein Mini Kit (Qiagen) and used for first strand cDNA synthesis using random primers and SuperscriptIII Reverse Transcriptase (Invitrogen). Quantitative real-time PCR (qRT-PCR) was performed using the following pre-validated TaqMan Assays (Applied Biosystems); PTBP1: Hs00738538, ANXA7-I1: Hs00244504, ANXA7-I2: Hs00559416, 18srRNA: Hs99999901, miR-124: TM2197. A TaqMan Human Angiogenesis 96-well Array (Applied Biosystems) was used for detection of angiogenesis markers. qRT-PCR with SYBR green (Applied Biosystems), and primers listed in Table S2, were used to validate selected angiogenesis markers.

EGF Stimulation, CHX Treatment, Immunoblotting, and Immunostaining

SNB19 cells were serum starved for 24 h in 0.2 % FBS and stimulated with EGF (50 ng/ml) for 30, 60, 90 or 120 min. For protein stability analysis, transduced SNB19 cells were treated with 100 μg/ml of cycloheximide (CHX) (Sigma) for 0, 30, 60, 120, 150,

180, or 210 min. The following antibodies were used in immunoblotting analyses: PTBP1 (rabbit polyclonal, MBL), ANXA7 (mouse monoclonal, Santa Cruz), EGFR (rabbit polyclonal, Santa Cruz), pEGFR (Y1068, rabbit polyclonal, Invitrogen), ERK1/2 (rabbit polyclonal, Abcam), pERK1/2 (pTyr202/Tyr204, mouse monoclonal, Assay designs), AKT1/2/3 (rabbit polyclonal, Santa Cruz), pAKT1/2/3 (rabbit polyclonal, Santa Cruz), β-actin (mouse monoclonal, Sigma) and α-tubulin (mouse monoclonal, Abcam). Primary antibodies were used at the concentration indicated by the manufacturers. Anti-Mouse and anti-Rabbit HRP-conjugated (Santa Cruz, dilution: 1:5000) were used as secondary antibodies. Immunostaining was performed using antibody against: PTBP1 (rabbit polyclonal, MBL), EGFR (mouse monoclonal, Millipore), EEA1 (rabbit polyclonal, Abcam), M6PR (rabbit polyclonal, Abcam), MMP9 (rabbit polyclonal, Cell Signaling), VEGF (rabbit, polyclonal, Thermo Scientific), Vimentin (mouse monoclonal, Sigma), PECAM1 (goat polyclonal, Santa Cruz), α-SMA (mouse monoclonal, Sigma). Primary antibodies were used at the concentration indicated by the manufacturers. Anti-Mouse, anti-Rabbit and anti-Goat Alexa594- or Alexa647-conjugated (Life Technologies) were used as secondary antibodies. Alexa594-conjugated antibodies were used at 1:200 dilution, Alexa647-conjugated antibodies were used at 1:100 dilution. Secondary labeling of anti-MMP9, VEGF, PECAM1 and α-SMA antibodies was performed by using the Tyramide Signal Amplification Kit (PerkinElmer) according to the manufacturer's instructions. Briefly, primary antibodies were labeled with the appropriate HRP-conjugated secondary antibody (dilution: 1:500) and then their signal was enhanced with the TSA Fluorophore Amplification Reagent provided in the kit. Pictures were acquired using an Axiovert Microscope (Carl Zeiss) or a FSL confocal microscope (Olympus).

Axiovision AXIOVS40 V4.8.0.0 (Carl Zeiss) or Fluoview FV10-ASW3.1 (Olympus) software was used for image processing and quantifications.

Pyrosequencing and Conventional Sequencing

For pyrosequencing analysis of ANXA7 exon 6 and the flanking intron/exon junctions, a genomic region was amplified by PCR using the following primers: forward: 5'-GGCTGGGTGATTGGTATTTC-3, reverse: 5'-GAGAATCAGAAACAAAGGCACA-3'. PCR products were purified using Sepharose beads and processed to yield single-stranded DNA as recommended by the manufacturer using the PyroMark Vacuum Prep Tool (Qiagen) and annealed to 0.3 μM pyrosequencing primer at 80°C. The sequence of the pyrosequencing primer was: 5'-CAGGATAGGAAGAAAAAG AATCTGTA-3'. Sequence analysis was performed using the manufacturer provided software (Qiagen) with default setting. We further sequenced a DNA segment from 161-bp upstream to 278-bp downstream of exon 6 via conventional sequencing on a 3730 DNA Analyzer (Applied Biosystems) using the following primers: forward: 5'-ACCTGGGGTCTTGGTTTTAGTT-3', reverse: 5'-CCAACAGTGAAACTCCATCTCA-3'. Data analysis was performed in BioEdit Software Version 7.0.9 (Ibis Biosciences).

RNA Immunoprecipitation (RNA-IP)

RNA-IP was performed in MB003 primary cell line infected with lentivirus expressing scrambled, non-targeting shRNA or PTBP-targeting shRNA using the RIP assay kit PTBP1 (MBL) according to the manufacturer's instructions. The co-precipitated RNA was transcribed to produce cDNA using random primers and SuperscriptIII Reverse

Transcriptase (Invitrogen). ANXA7 was amplified by PCR using the following primers:

hANXA7-Exon6-Sen6: ACCTGGGGTCTTGGTTTTAGTT

hANXA7-Exon6-Rev6: CCAACAGTGAAACTCCATCTCA

ExonTrap Assay

A minigene including the genomic sequence between *ANXA7* exon5 and exon7 (ANXA7E5-7) was cloned into an ExonTrap vector (MoBiTec) and transfected into SNB19 cells expressing control or PTBP1 shRNA. The mature RNA was transcribed to produce exogenous specific cDNA according to the manufacturer's instructions. *ANXA7* splicing was measured by PCR using primers specific for the ectopic cDNA:

ANXA7for: TGTGGTTCTCACTTGGTGGA

ANXA7rev: GTGCCACAAAACCCTTCATT

PTBP1 Binding Site Prediction and Site-Directed Mutagenesis

PTBP1 binding site predictions were performed using PTB-CLIP-seq data from Xue *et al*. and (2, 3) and next-generation systematic evolution of ligands by exponential enrichment (SELEX) by Reid *et al*. (4) as described in (5). The class of PTB binding sequences was derived from the set of 51.394 peaks. Analogous to the original publication, additional 25nt were added to each side of the peaks. The set of non-binding sequences was derived by shuffling the locations of the binding sites within the genome under the following constraints: Negative sites had to be located within introns and were not allowed to fall within 125 nucleotides of any CLIP-seq read. For model creation, secondary structures were computed using RNAshapes (6) employing shape abstraction

level 3 and sliding windows of sizes 50 and 100. Feature vectors for model training were computed with the NSPD Kernel using subgraphs of radius 3 and distance 6. Training of the binding model was done using stochastic gradient descent (SGD). This model was used to score each nucleotide of the ANXA7 minigene as well as the suggested mutations for the suppression of PTB-binding. Using the nucleotide-wise scores, we extracted a set of 10 high-scoring binding-site candidates. To disable PTB binding at these sites we computed sets of 1-7 mutations causing the largest reduction of the overall scores according to the model. To this end, we used an iterative *k*-best search in which we added one extra mutation for every iteration. A single mutation will cause changes of secondary structure, which in turn will influence the scores of the other nucleotides. By first evaluating the changes introduced by another mutation, we ensure that changes are introduced only where really needed. Starting from the set of n lowest ranking candidates from the previous iteration (the original sequence for the first iteration) we introduced additional mutations at the *k* highest-scoring nucleotides, each mutation forming a new candidate sequence. The sequence having the lowest score among the candidates was chosen as the representative for this iteration. Mutations for this work were computed using parameters $k = n = 10$. Site-directed mutagenesis was performed using the QuikChange II Site-Directed Mutagenesis kit (Agilent) according to the manufacturer's instructions. Primers are listed in Table S3.

Probed Isoelectric Focusing (PIF) Analysis

SNB19 cells were serum starved for 24 h in 0.2 % FBS and stimulated with EGF (50 ng/ml) for 30 or 60 min. Cells were lysed in RIPA buffer containing phosphatase and

protease inhibitors (ProteinSimple). Samples were run in triplicate. Lysates (2 μg/μl) were mixed with ampholyte premix (pH 5–8) and fluorescent pI standards (pI Standard Ladder 3) before being loaded into the NanoPro100 system (ProteinSimple) for analysis. The mix was loaded in capillaries to perform isoelectric focusing. The separated proteins were cross-linked to the capillary wall using UV light followed by immunoprobing with anti-EGFR (Y1068) (Abcam) or anti-ERK1/2 (ProteinSimple). Anti–rabbit HRP-conjugated secondary antibody (ProteinSimple) was used to detect the signal. The signal was visualized by ECL and was captured by a charge-couple device camera. The digital image was analyzed and peak area quantified with Compass software (ProteinSimple).

Migration and Invasion Assays

For the wound-healing assay, SNB19 cells infected with lentivirus were plated in 60 mm dishes and grown at 95% confluence. A scratch of approximately 1 mm was made with a p1000 pipette tip and images were taken every 10-12 hours using a wide-field microscope (Axiovert, Zeiss). The Matrigel invasion assay was done using BioCoat Matrigel Invasion Chambers (BD Bioscience) according to the manufacturer's instructions. $2.5x10^4$ cells infected with lentivirus were seeded in the upper compartment. PDGF-BB (20ng/ml, R&D) was used as a chemoattractant.

Senescent Assay

β-Gal staining of senescent cells was done using the Senescence Detection kit (Calbiochem) according to the manufacturer's instructions. Each sample was run in triplicate and pictures of the entire wells were taken using the Axioplan2 Imaging system

(Carl Zeiss) with MosaiX Axiovision software (Carl Zeiss). β-Gal positive cells were counted by randomly selecting 5 regions of the same size across each mosaic reconstruction.

Intracranial Injection

Intracranial injection of SNB19 glioblastoma cells or BTSC23 cells was performed in groups of 6-8 NOD/SCID mice (Charles River laboratories) in accordance with the Directive 86/609/EEC of the European Parliament, following approval by the ethics review board for animal studies at the University of Freiburg. Experiments were performed as described earlier (7). Briefly, after dissociation, SNB19 ($5x10^5$) or BTSC-23 ($3x10^5$) cells infected with lentivirus were injected intra-parenchymally into the frontal lobe at 0.5 mm anterior and 2 mm lateral from the bregma to a depth of 3 mm in the brain using a Hamilton syringe fixed to a stereotactic frame. Animals were followed by visual inspection and sacrificed if found to demonstrate any signs of neurological decline.

Xenograft Tumor Collection and Processing

For histological analysis, brains were removed, placed into 4% paraformaldehyde fixative overnight and embedded in paraffin before staining with hematoxylin and eosin (H&E) or immunostaining was performed. Pictures were acquired using an Axioplan2 Imaging system (Carl Zeiss) with MosaiX Axiovision software (Carl Zeiss) or using a FSL confocal microscope (Olympus).

Small Animal MRI Analysis

For detection of the injection site, high-resolution brain imaging was performed 7 days after intracranial injection. Experiments were performed at 7 T on a Bruker Biospec System. A cryogenically-cooled quadrature-resonator (Bruker, Ettlingen, Germany) was used as transceiver. High-resolution multislice 2D gradient echo flow compensated images were acquired with the following parameters: *TR* = 1000 ms, *TE* = 16 ms, flip angle = 72 degrees, resolution 35 x 35 x 250 μm^3, within a short acquisition time of 7 min; the flip angle was adjusted to Ernst angle considering T_1 = 1600 ms (mouse cerebral cortex). Images were processed offline with custom-made software developed in Matlab to reconstruct both T2-weighted magnitude and phase images. After Fourier transformation, in order to preserve the phase information, the complex images acquired with each individual channel were combined using the adaptive reconstruction method proposed by Walsh *et al*. (8). The background field inhomogeneity resulting from imperfect shimming was removed by applying a low pass filter of the complex image (Gaussian filter equal to the image size) followed by the complex division of the complex image by the low pass filtered image on a voxel by voxel basis. The resulting phase images preserve the small-scale phase variations caused by the presence of the tumor cells (bright spots) yielding higher contrast compared to the host tissue. For detection of BTSC23-derived tumors, T2-weighted images were acquired using a multislice RARE sequence with: TR = 3600 ms, TE = 36 ms, resolution 85 × 85 × 500 μm3, T_{scan} = 8 min 38 s.

Gene Co-Regulation Analysis

Spearman's rank correlation coefficients between the expression of PTBP1 and EGFR and angiogenesis genes were computed on a genome-wide scale using Matlab and co-expression was deemed significant based on false-discovery rate estimation with a q of $< 10^{-3}$. Significantly co-expressed transcripts were mapped on a circular human genome structure using Circos (http://circos.ca/).

Endothelial Cell Tube Formation Assay

Human Umbilical Vein Endothelial Cells (HUVEC) (Millipore) were seeded in Matrigel-covered (10mg/ml; 200 μl/well) 24-well plates at a concentration of 80000 cells/well and incubated 24 hours with 500 μl of complete Neurobasal medium conditioned by BTSCs for the previous 48 hours. Erlotinib treatment was performed by adding 1μM Erlotinib Hydrochloride (Santa Cruz) to the complete Neurobasal medium during the 48-hour incubation with the BTSCs. Bevacizumab (2.5 mg/ml; Genentech/Roche) was added directly into the conditioned medium when the HUVECs were exposed to it. Triplicates of each sample group were imaged with an Axiovert Microscope (Carl Zeiss) at 2.5X magnification. Images were processed and quantified with Axiovision AXIOVS40 V4.8.0.0 (Carl Zeiss).

Statistic Analyses

Linear regression analyses and graphical model validation were executed using R software. Scatterplots and locally weighted least squares (LOWESS) smooths were used to confirm the suitability of linear regression analyses, and statistical significance of these

relationships was assessed according to the p value for the estimated slope of the regression line. A multiple linear regression model was computed based on the ordinary least squares method. Survival curves were estimated by the Kaplan-Meier product-limit method, and survival distributions were compared across groups using the log-rank test. Unpaired t-test and Wilcoxon rank-sum test were used as appropriate. p values < 0.05 were considered significant, except for linear regression analysis of co-regulated expression of PTBP1 and EGFR with multiple angiogenesis genes, in which a false-discovery rate a adjusted q value < 0.001 was considered significant.

Study Approval

Human studies were approved by the Institutional Review Boards of Stanford University and Northwestern University, and by the Ethics Committee of the University of Freiburg. Animal studies were approved by the Animal Review Committee of the University of Freiburg.

SUPPLEMENTAL REFERENCES

1. Mermel, C.H., Schumacher, S.E., Hill, B., Meyerson, M.L., Beroukhim, R., and Getz, G. 2011. GISTIC2.0 facilitates sensitive and confident localization of the targets of focal somatic copy-number alteration in human cancers. *Genome Biol* 12:R41.
2. Xue, Y., Zhou, Y., Wu, T., Zhu, T., Ji, X., Kwon, Y.S., Zhang, C., Yeo, G., Black, D.L., Sun, H., et al. 2009. Genome-wide analysis of PTB-RNA interactions reveals a strategy used by the general splicing repressor to modulate exon inclusion or skipping. *Mol Cell* 36:996-1006.

3. Xue, Y., Ouyang, K., Huang, J., Zhou, Y., Ouyang, H., Li, H., Wang, G., Wu, Q., Wei, C., Bi, Y., et al. 2013. Direct conversion of fibroblasts to neurons by reprogramming PTB-regulated microRNA circuits. *Cell* 152:82-96.
4. Reid, D.C., Chang, B.L., Gunderson, S.I., Alpert, L., Thompson, W.A., and Fairbrother, W.G. 2009. Next-generation SELEX identifies sequence and structural determinants of splicing factor binding in human pre-mRNA sequence. *RNA* 15:2385-2397.
5. Maticzka, D., Lange, S.J., Costa, F., and Backofen, R. 2014. GraphProt: modeling binding preferences of RNA-binding proteins. *Genome Biol* 15:R17.
6. Giegerich, R., Voss, B., and Rehmsmeier, M. 2004. Abstract shapes of RNA. *Nucleic Acids Res* 32:4843-4851.
7. Carro, M.S., Lim, W.K., Alvarez, M.J., Bollo, R.J., Zhao, X., Snyder, E.Y., Sulman, E.P., Anne, S.L., Doetsch, F., Colman, H., et al. 2010. The transcriptional network for mesenchymal transformation of brain tumours. *Nature* 463:318-325.
8. Walsh, D.O., Gmitro, A.F., and Marcellin, M.W. 2000. Adaptive reconstruction of phased array MR imagery. *Magn Reson Med* 43:682-690.